

6<sup>th</sup> Intercontinental Geoinformation Days

igd.mersin.edu.tr



## Rapture and surface deformation mapping of Türkiye 2023 earthquake using DInSAR with Sentinel-1 satellite data

Pouya Mahmoudnia<sup>\*1</sup>, Mohammad Sharifikia <sup>1</sup>

<sup>1</sup>Tarbiat Modares University, Faculty of Humanities, Department of Remote Sensing and GIS, Tehran, Iran

### Keywords

Remote sensing  
DInSAR  
Geo-Hazard  
Earthquake

### Abstract

This paper showcases the utility of the Differential Interferometric Synthetic Aperture Radar (DInSAR) technique in mapping the surface deformation caused by the 7.8  $M_w$  earthquakes that hit the southern pate of Türkiye on February 6, 2023. By processing SAR data acquisition by Sentinel-1A satellite. The study result demonstrates the ability of DInSAR to provide highly accurate and comprehensive information on rapture caused over the known fault as well as jolting and land deformation area from strong seismic events. Furthermore, the observed significant surface deformation, including both uplift and subsidence, highlights the potential of DInSAR in geo-hazard study which can mitigate the risk and disaster caused by earthquakes. The results underline the importance of real-time earthquake detection and monitoring and can do early warning to the policies and other emergencies time to save life as more as possible close to the shake.

## 1. Introduction

Earthquakes are damaging geo-hazard that affect many people each year. Real-time earthquake detection and monitoring are vital for mitigating loss of life and property damage.

Differential Interferometric Synthetic Aperture Radar (DInSAR) is an effective remote sensing technique for seismic detection and monitoring. It provides comprehensive data on ground alterations and surface dislocation from seismic events (Vaka et al. 2021; Vaka et al. 2020; Xu et al. 2020).

On February 6, 2023, a 7.8  $M_w$  earthquake hit southern Türkiye, followed by a 7.5  $M_w$  earthquake about 90km to the north 9 hours later. The epicenters of these earthquakes are shown in Figure 1. The 7.8  $M_w$  earthquake and its aftershocks occurred in the transition zone between the Dead Sea and East Anatolian faults, while the epicenter of the 7.8  $M_w$  earthquake was located near the triple junction of the Arabian, African, and Anatolian plates. The Anatolian fault moves Türkiye toward the Aegean Sea, while the Dead Sea fault moves Arabia northward on the African plate.

In this study, we employed the Differential Synthetic Aperture Radar Interferometry (DInSAR) technique to

cartographically depict the seismic surface deformation that resulted from the 7.8  $M_w$  earthquake of 2023 using Sentinel-1 satellite data.

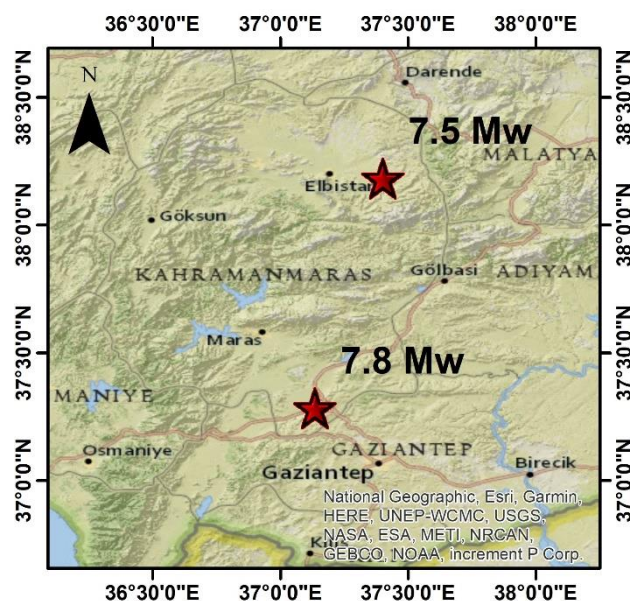


Figure 1. The epicenters of the earthquakes

\* Corresponding Author

<sup>\*</sup>(po.mahmoudnia@gmail.com) ORCID ID 0009-0000-5189-8429  
(sharifikia@modares.ac.ir) ORCID ID 0000-0003-3563-8816

Cite this study

Mahmoudnia P & Sharifikia M (2023). Rapture and surface deformation mapping of Türkiye 2023 earthquake using DInSAR with Sentinel-1 satellite data. Intercontinental Geoinformation Days (IGD), 6, 302-304, Baku, Azerbaijan

## 2. Data and Method

### 2.1. Data

The present study employed SAR imagery derived from the European Space Agency's (ESA) C-band Sentinel-1 data, obtained from both ascending and descending orbits in the VV polarization (i.e., vertical transmit and vertical receive), to delineate the topographic changes resulting from the earthquake. The data was collected before and after the seismic event (see Table 1).

**Table 1.** Satellite dataset information used in this study

Items	Ascending	Descending
Master	2023/01/28	2023/01/29
Slave	2023/02/09	2023/02/10
Baseline(m)	168.324	106.558
Incidence angle	43.92°	39.39°

### 2.2. Method

DInSAR is a technique that employs Synthetic Aperture Radar (SAR) images to measure land deformation by comparing two or more radar images taken at different times. Images are processed to obtain an interferogram, showing phase differences between two radar images caused by changes in ground displacement.

The total differential phase difference ( $\Delta\phi$ ) through fringes that account for various factors, including topography ( $\phi_{\text{topo}}$ ), orbital fringe or baseline ( $\phi_{\text{orbit}}$ ), and movement ( $\phi_{\text{mov}}$ ) caused by natural occurrences such as seismic or aseismic activities. Additionally, the representation incorporates fringes originating from atmospheric effects ( $\phi_{\text{atmos}}$ ) and phase noise ( $\phi_{\text{noise}}$ ).

$$\Delta\phi = \phi_{\text{topo}} + \phi_{\text{orbit}} + \phi_{\text{mov}} + \phi_{\text{atmos}} + \phi_{\text{noise}}$$

ALOS WORLD 3D-30m (AW3D30 DEM) is used to remove topographic fringes in interferograms. To reduce phase error caused by decorrelation, using an adaptive filter can enhance phase quality. We applied an adaptive filter, a modified version (Baran et al. 2003) of Goldstein's filtering method (Goldstein and Werner, 1998). After phase unwrapping, we refined the orbital parameters by selecting control points across interferograms to eliminate phase ramps. The unwrapped phase values were converted into line of sight (LOS) displacement and geocoded into a map projection. All procedures were executed utilizing the SARscape 5.4.1 software.

## 3. Results and Discussion

The interferograms resulting from the earthquakes, acquired via Sentinel-1 ascending and descending data, are depicted in Figure 2 and Figure 3. Each individual fringe correlates with a complete cycle of phase variation and corresponds to a displacement of 2.8 centimeters in line-of-sight (LOS) in C-band interferograms.

The observed interferograms exhibit intricate and dense fringes. The patterns observed on the fringes exhibit inverse characteristics in terms of their densities and contrasts.

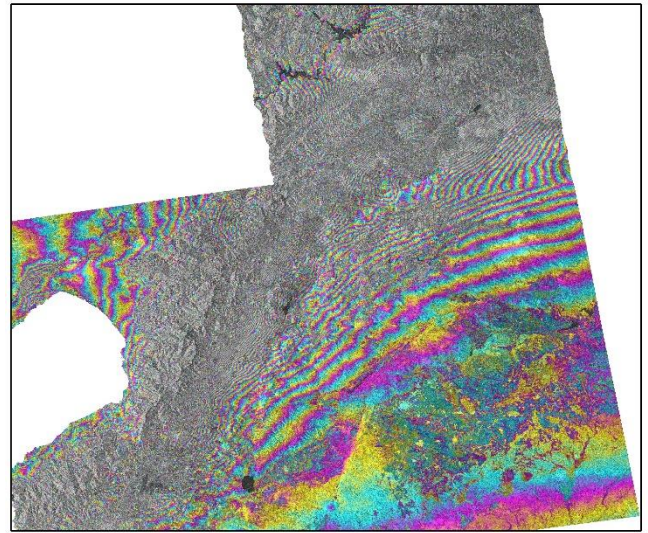


**Figure 2.** Interferogram of the Ascending pair

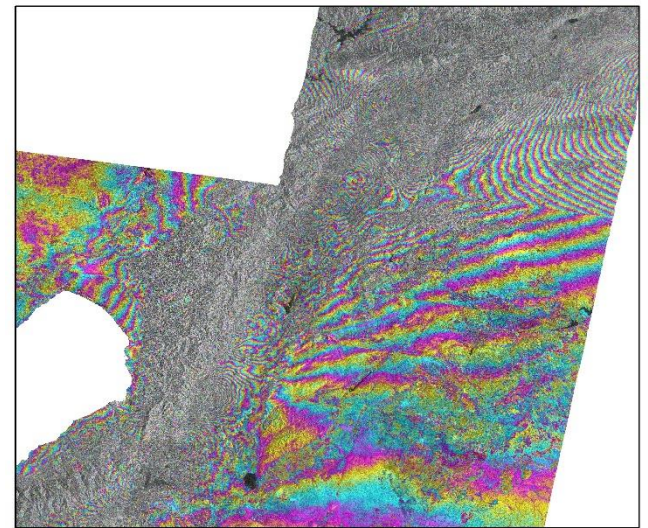


**Figure 3.** Interferogram of the descending pair

The figures presented in Figure 4 and Figure 5 illustrate LOS displacement maps. The observations indicate that the Sentinel-1 ascending data recorded a displacement of 1.68 m for uplift and -1.26 m for subsidence. Similarly, the Sentinel-1 descending data recorded a displacement of 1.08 m for uplift and -1.42 m for subsidence. The differences observed in the maximum and minimum displacements between the two measurements appear to be the result of alterations in the satellite pass and look direction. The standard deviation values for the observed displacements were determined to be 0.29 and 0.23 meters for the Sentinel-1 ascending and Sentinel-1 descending data sets, respectively.

## 4. Conclusion

In conclusion, the present study demonstrated the effectiveness of Differential Interferometric Synthetic Aperture Radar (DInSAR) as a remote sensing technique for seismic detection and monitoring, using Sentinel-1 satellite data to analyze the surface deformation resulting from the February 6, 2023 earthquake in southern Türkiye. The observed significant surface

deformation, including both uplift and subsidence, highlights the potential of DInSAR in mitigating the loss of life and property damage caused by earthquakes. The study provides valuable insights into the use of DInSAR for real-time earthquake detection and monitoring, which can aid in disaster preparedness and response efforts. Further research in this area can help to improve our understanding of the impact of earthquakes on the earth's surface and inform policies and strategies for earthquake risk reduction.

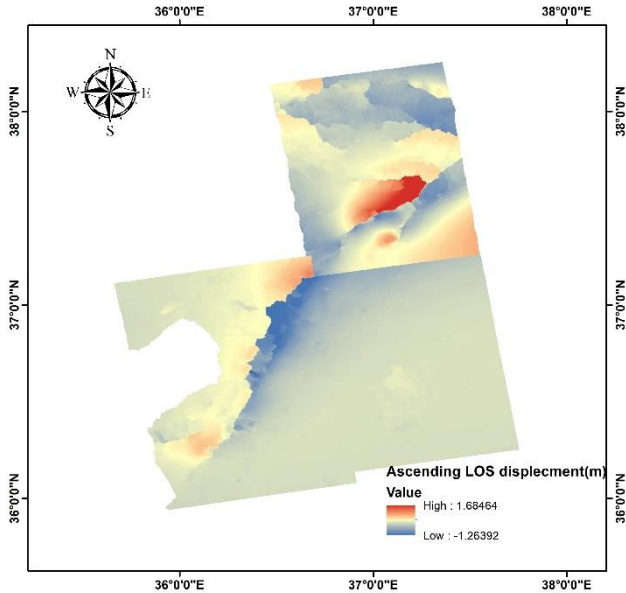


**Figure 4.** LOS displacement of the ascending pair

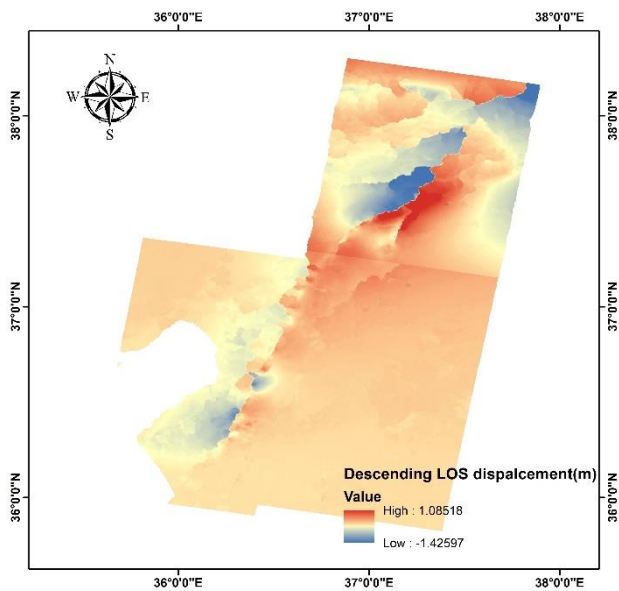


**Figure 5.** LOS displacement of the descending pair

## References

- Baran, I., Stewart, M. P., Kampes, B. M., Perski, Z., & Lilly, P. (2003). A modification to the goldstein radar interferogram filter. *IEEE Transactions on Geoscience and Remote Sensing*, 41(9 PART II), 2114–2118. <https://doi.org/10.1109/TGRS.2003.817212>
- Goldstein, R. M., & Werner, C. L. (1998). Radar interferogram filtering for geophysical applications. *Geophysical Research Letters*, 25(21), 4035–4038. <https://doi.org/10.1029/1998GL900033>
- Vaka, D. S., Rao, Y. S., & Bhattacharya, A. (2021). Surface displacements of the 12 November 2017 Iran–Iraq earthquake derived using SAR interferometry. *Geocarto International*, 36(6), 660–675. <https://doi.org/10.1080/10106049.2019.1618927>
- Vaka, D. S., Rao, Y. S., & Singh, T. (2020). Surface deformation of the 2019 mirpur earthquake estimated from sentinel-1 insar data. *2020 IEEE India Geoscience and Remote Sensing Symposium, InGARSS 2020 - Proceedings*, 130–133. <https://doi.org/10.1109/InGARSS48198.2020.9358915>
- Xu, X., Sandwell, D. T., & Smith-Konter, B. (2020). Coseismic displacements and surface fractures from sentinel-1 InSAR: 2019 Ridgecrest earthquakes. *Seismological Research Letters*, 91(4), 1979–1985. <https://doi.org/10.1785/0220190275>